

relation $\vec{k}_0 = \vec{k} + \vec{k}'$, where \vec{k} or \vec{k}' refer to the originally unstable modes. Two instabilities for which the instability criteria are met in the current sheath have angular dependences similar to those observed. They are the electron-cyclotron drift instability⁴ and the lower-hybrid drift² instability.

The authors are grateful for helpful discussions with H. R. Griem, N. A. Krall, and R. C. Davidson and for the technical assistance of W. Knouse and K. Diller.

*Work supported by the U. S. Office of Naval Research.

¹*Proceedings of the Fourth International Conference on Plasma Physics and Controlled Nuclear Fusion Research, Madison, Wisconsin, 1971* (International Atomic Energy Agency, Vienna, 1971), Vol. III.

²N. A. Krall and P. C. Liewer, *Phys. Fluids* **15**, 1166 (1972).

³K. Papadopolous, R. C. Davidson, J. M. Dawson, I. Haber, D. A. Hammer, N. A. Krall, and R. Shanny, *Phys. Fluids* **15**, 849 (1971).

⁴D. Forslund, R. Morse, C. Nielson, and J. Fu, *Phys. Fluids* **15**, 1303 (1972).

⁵M. Lampe, W. M. Manheimer, J. B. McBride, J. H. Orens, K. Papadopolous, R. Shanny, and R. N. Sudan, *Phys. Fluids* **15**, 662 (1972).

⁶A. W. DeSilva and G. C. Goldenbaum, in *Methods of Experimental Physics*, edited by H. R. Griem and R. Lovberg (Academic, New York, 1969), Vol. 9.

⁷H. W. Drawin, *Z. Phys.* **225**, 470 (1969).

⁸C. C. Daughney, L. S. Holmes, and J. W. M. Paul, *Phys. Rev. Lett.* **25**, 497 (1970).

⁹M. Kornherr, G. Decker, M. Keilhacker, F. Lindenberg, and H. Rohr, *Phys. Lett.* **39A**, 95 (1972).

¹⁰H.-J. Kunze, H. R. Griem, A. W. DeSilva, G. C. Goldenbaum, and I. J. Spalding, *Phys. Fluids* **12**, 2669 (1969).

¹¹A. W. DeSilva, W. F. Dove, I. J. Spalding, and G. C. Goldenbaum, *Phys. Fluids* **14**, 42 (1971).

¹²O. Buneman, *Phys. Rev.* **115**, 503 (1959).

Propagation of Fourth Sound in Superfluid ³He†

H. Kojima, D. N. Paulson, and J. C. Wheatley

Department of Physics, University of California at San Diego, La Jolla, California 92037

(Received 16 November 1973)

Pressure waves propagate through a superleak in both ³He-A and ³He-B, showing that both are superfluids below T_c . Superfluid relative density is obtained from velocity measurements over a wide pressure range above and below the polycritical point.

We have shown using both transient and resonance methods that pressure waves propagate through a superleak in both ³He-A and ³He-B over a wide range of static pressure.¹ This is the first experimental proof of the superfluidity of both extraordinary phases of liquid ³He. Fourth sound, a pressure wave in superfluid ⁴He with normal fluid locked in a porous medium, was first discussed by Pellam² and observed by Rudnick and Shapiro.³ It has been discussed theoretically in a context of ³He by de Gennes⁴ and Saslow.⁵ Measurements of fourth-sound velocity C_4 yield relative superfluid density $\bar{\rho}_s/\rho$ via the equation

$$\bar{\rho}_s/\rho = C_4^2/C_1^2, \quad (1)$$

where C_1 is the velocity of first sound⁶ and $\bar{\rho}_s/\rho$ denotes a suitable average if the superfluid is anisotropic or if size effects are important, and where thermal effects³ have been neglected with sufficient accuracy for present purposes. Our measurements, extending down to $T/T_c \approx 0.8$,

show that $\bar{\rho}_s/\rho$ is quite small, varies slowly with temperature, and shows little or no detectable change near the first-order transition at T_{AB} ; this is in possible disagreement with the interpretation of the wire-damping experiments⁷ and with a prediction⁸ relating $1 - \rho_s/\rho$ and zero-sound velocity, but is reasonably close to what one might expect from susceptibility⁹ measurements.

Our experimental epoxy cell, 2.63 cm long and 2.11 cm in diameter, was packed with cerium magnesium nitrate (CMN) powder (size less than 37 μm) to 80% of crystalline density, the CMN being used as superleak, refrigerant, and thermometer. Each end was closed using a capacitive-type pressure transducer.³ For transient measurements a voltage step of 20–40 V was applied to the transmitting transducer; the receiving transducer was connected through a band-limiting amplifier to an oscilloscope. For resonance measurements the transmitter was driven by the reference channel of a lockin detector; the receiver was connected to a preamplifier

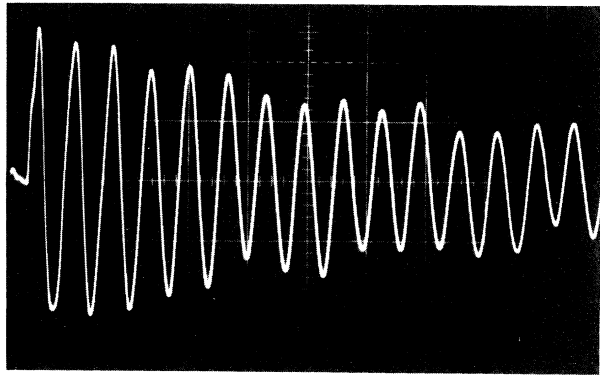


FIG. 1. Response of receiving transducer to a step applied to the transmitting transducer showing the initial transit time and subsequent echoes of fourth sound for a pressure of 25.5 bar and $T/T_c = 0.89$. The receiving bandwidth is $300-10^3$ Hz, the horizontal sweep is 2 msec per main division, and twice the cell length is 5.25 cm.

and then to the lockin. For ^4He measurements at low T the cell had a $Q > 500$, but for the ^3He measurements the amplitude, though not the frequency, of the fourth-sound signal was history dependent and sensitive to pulse heating. We were unable to obtain information on intrinsic dissipation, not unlike fourth-sound measurements with ^4He .³

Typical response of the receiving system (bandwidth $300-10^3$ Hz) to a 40-V step at the transmitter is shown in Fig. 1. The step occurs at the extreme left of the trace; the receiver responds as shown, the time separation between adjacent maxima being the same within experimental precision as the reciprocal of the frequency of the corresponding fundamental resonance.

Precise measurements of $\bar{\rho}_s/\rho$ were obtained as a function of temperature by measuring the first longitudinal resonance¹⁰ frequency f . Because of the reduction of the measured fourth-sound velocity from that calculated using Eq. (1) by the effective index of refraction³ of the powder, we obtained $(\bar{\rho}_s/\rho)_{^3\text{He}}$ using the equation

$$\left(\frac{\bar{\rho}_s}{\rho}\right)_{^3\text{He}} = \frac{[(f/C_1)_{^3\text{He}}]^2}{[(f/C_1)_{^4\text{He}, T=0}]^2}, \quad (2)$$

where the denominator was determined¹¹ by separate experiments at pressures from zero to the melting-curve minimum with the same mode in the same cell but with superfluid ^4He near $T = 0$, where $(\rho_s/\rho)_{^4\text{He}}$ is unity. Some of our measurements are shown in Fig. 2 as $\bar{\rho}_s/\rho$ calculated from the experimental quantities in Eq. (2) ver-

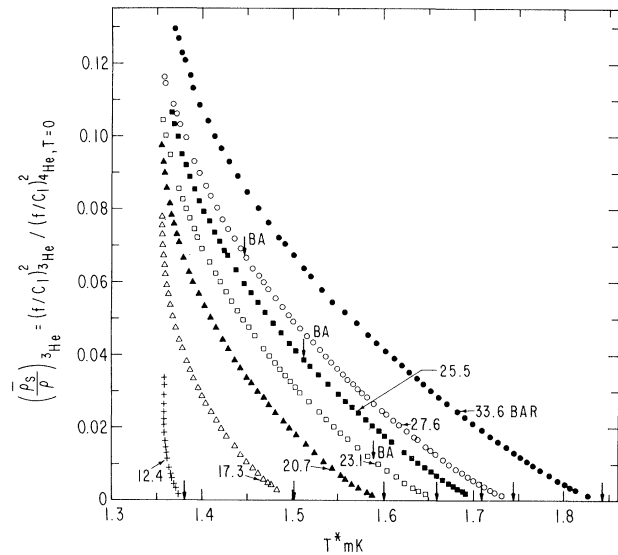


FIG. 2. Experimental values of $\bar{\rho}_s/\rho$ obtained using Eq. (2) as a function of CMN magnetic temperature for 33.59 (filled circles), 27.56 (open circles), 25.50 (filled squares), 23.09 (open squares), 20.69 (filled triangles), 17.26 (open triangles), and 12.39 (plus signs) second-order transition temperatures T_c^* are indicated by arrows on the horizontal axis. The expected locations of T_{AB}^* are shown by arrows on the appropriate curves. The polycritical point is at ~ 21.7 bar.

sus the CMN magnetic temperature T^* . The phenomenon of a minimum magnetic temperature as absolute temperature T decreases is evident. The critical temperatures T_c^* were obtained thermally¹² for $P > 14$ bar and at lower pressures by extrapolating $\bar{\rho}_s/\rho$ to zero and are shown by arrows along the axis in Fig. 2. The arrows marked BA on Fig. 2 for pressures of 27.56, 25.50, and 23.09 bar (all above the polycritical point) are the expected positions of the $B-A$ transition according to our susceptibility measurements.⁹ Although we expect from experience that $^3\text{He}-B$ would have formed for these pressures, there is no major change at T_{AB}^* evident either on this plot or, more sensitively, on plots like that of Fig. 3. Changes, if any, in $\bar{\rho}_s/\rho$ at T_{AB} are less than 5-10% as measured in this experiment.

By measuring T_c^* for ten pressures and comparing with the $P-T_c$ curve based primarily on our zero-sound measurements,⁶ we obtained a $T-T^*$ relation for the present thermometer which we used to make reduced plots of $\ln \bar{\rho}_s/\rho$ versus $\ln(1 - T/T_c)$. These show little pressure dependence (probably less than 10%) and are sensitive to uncertainties both in T_c and in the $T-T^*$ relation. An example is shown in Fig. 3 for a pres-

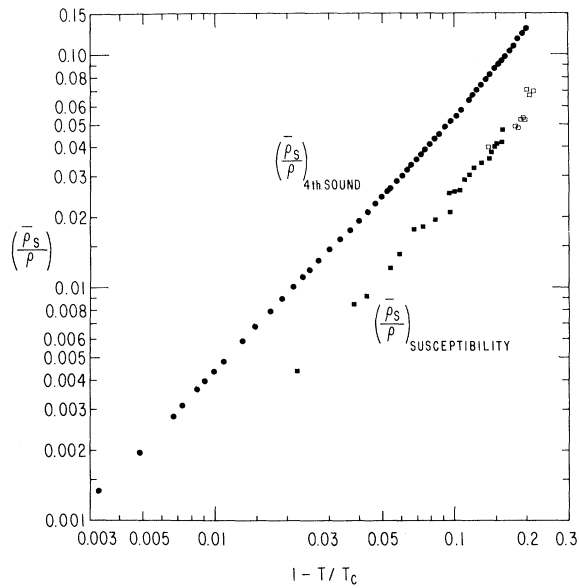


FIG. 3. Logarithmic plot of $\bar{\rho}_s/\rho$ versus $1 - T/T_c$ for a pressure of 33.59 bar (circles). Also shown are the values of $\bar{\rho}_s/\rho$ deduced from susceptibility measurements of Ref. 8 via Eqs. (3) and (4) for pressures of 20.8 (filled squares) and 29.9 bar (open squares), assuming the pressure independence of reduced plots.

sure of 33.59 bar, for which the liquid is entirely in the $^3\text{He-A}$ state. The data for all pressures are not badly represented by $\bar{\rho}_s/\rho \propto (1 - T/T_c)^\alpha$ with α in the range 1.1–1.3, although quantitative conclusions are weak because of uncertainties in the temperature scale and in the precise value of T_c and the possibility of size effects.¹³ With respect to the latter, experiments with a more open structure are now being contemplated.

Excluding Fermi-liquid effects, in weak-coupling theory for nonmagnetic pairs¹⁴ both the reduced nuclear susceptibility χ/χ_n , where χ_n is the nuclear susceptibility of the normal state, and $1 - \bar{\rho}_s/\rho$ are the same function $g(T/T_c)$, whether the superfluid is isotropic or not. Including Fermi-liquid effects, Leggett showed¹⁴ that for $L = 0$ pairing, one has

$$\frac{\chi}{\chi_n} = \frac{(1 + \frac{1}{4}Z_0)g(T/T_c)}{1 + \frac{1}{4}Z_0g(T/T_c)}, \quad (3)$$

and

$$\left(1 - \frac{\bar{\rho}_s}{\rho}\right) = \frac{(1 + \frac{1}{3}F_1)g(T/T_c)}{1 + \frac{1}{3}F_1g(T/T_c)}, \quad (4)$$

where Z_0 and F_1 are Fermi-liquid parameters.¹⁵ Although weak-coupling theory probably does not apply and the Fermi-liquid corrections given in Eqs. (3) and (4) are probably not accurate for L

> 0 pairing, we nevertheless hope to estimate $\bar{\rho}_s/\rho$ from experimental data for χ/χ_n using these formulas. We use the data of Ref. 8 and do not interpret $^3\text{He-B}$ as a Balian-Werthamer¹⁶ state since for the lowest T/T_c achieved there the value of χ/χ_n is much too low for that interpretation. We further assume approximate pressure independence and $^3\text{He-A}$ – $^3\text{He-B}$ independence of the data on a reduced plot. The resulting values of $\bar{\rho}_s/\rho$ are shown on Fig. 3. The agreement is not quantitative, but might be considered reasonable in that near T_c changes in χ/χ_n are divided by a factor $(1 + F_1/3)/(1 + Z_0/4) \sim 20$ to 25 to obtain the corresponding changes in $\bar{\rho}_s/\rho$.

The small values for $\bar{\rho}_s/\rho$ found in our experiment for $T/T_c > 0.8$ and the corresponding slight reduction in $\bar{\rho}_n/\rho$ for this temperature region as well as the small, if any, change in $\bar{\rho}_s/\rho$ at the A – B transition do not support the interpretation given by Alvesalo *et al.*⁷ of their wire-damping experiment, barring gross size effects and some special sensitivity to fluid anisotropy which would be undetectable in our experiment. It is possible that in this temperature range the two-fluid model need not be introduced at all to explain within experimental error their measurements for $T > 0.8T_c$, which then would reflect both a decreasing viscosity and nonlinear effects, in disagreement with Seiden's theory¹⁷ of viscosity but in qualitative agreement with heat-flow measurements.¹ Our measurements also disagree with the predictions of the phenomenological theory of Putterman, in which $1 - \rho_s/\rho$ should have the same temperature dependence as the reduced velocity of collisionless sound.¹² Nevertheless, our work must be interpreted with care since we measure an angularly averaged value $\bar{\rho}_s/\rho$, and in a packed powder susceptible to size effects rather than in bulk fluid.

We thank Professor S. J. Putterman for his part in the motivation of this experiment and Evelin Pichelmann for participation in preliminary work. We are grateful to Professor I. Rudnick for helpful discussions and to Professor A. L. Fetter and Professor Bruce Patton both for discussing this experiment with us and for quantitative help on its interpretation.

†Work supported by the U.S. Atomic Energy Commission under Contract No. AT(04-3)-34, P.A. 143.

¹T. J. Greytak, R. T. Johnson, D. N. Paulson, and J. C. Wheatley, Phys. Rev. Lett. **31**, 452 (1973). This paper defines notation via a phase diagram.

²J. R. Pellam, Phys. Rev. **73**, 608 (1948).

³K. A. Shapiro and I. Rudnick, Phys. Rev. **137**, A1383 (1965).

⁴P. G. de Gennes, Phys. Lett. **44A**, 271 (1973).

⁵W. M. Saslow, Phys. Rev. Lett. **31**, 870 (1973).

⁶D. N. Paulson, R. T. Johnson, and J. C. Wheatley, Phys. Rev. Lett. **30**, 829 (1973), and unpublished work.

⁷T. A. Alvesalo, Yu. D. Anufriyev, H. K. Collan, O. V. Lounasmaa, and P. Wennerström, Phys. Rev. Lett. **30**, 962 (1973).

⁸S. J. Putterman, Phys. Rev. Lett. **30**, 1165 (1973).

⁹D. N. Paulson, R. T. Johnson, and J. C. Wheatley, Phys. Rev. Lett. **31**, 746 (1973).

¹⁰The second longitudinal resonance occurred at a frequency only 1–2% greater than $2f$.

¹¹The quantity $(f/C_1)_{4\text{He}, T=0}$ varied from 0.088 at zero pressure to 0.081 on extrapolating the pressure measurements to 34 bar. Values of C_1 for ^4He were ob-

tained from B. M. Abraham, Y. Eckstein, J. B. Ketterson, M. Kuchnir, and P. R. Roach, Phys. Rev. A **1**, 250 (1970). At zero pressure the corresponding index of refraction is 2.16, rather different from the value of 1.34 expected from the empirical factor used in Ref. 3; however, both the powder and the packing are quite different from those used in Ref. 3.

¹²R. A. Webb, T. J. Greytak, R. T. Johnson, and J. C. Wheatley, Phys. Rev. Lett. **30**, 210 (1973).

¹³M. Kriss and I. Rudnick, J. Low Temp. Phys. **3**, 339 (1970).

¹⁴A. J. Leggett, Phys. Rev. **140**, A1869 (1965).

¹⁵See J. C. Wheatley, Physica (Utrecht) **69**, 218 (1973), for a recent compilation.

¹⁶R. Balian and N. R. Werthamer, Phys. Rev. **131**, 1553 (1963).

¹⁷J. Seiden, C. R. Acad. Sci., Ser. B **276**, 905 (1973).

Mass Diffusivity of ^3He - ^4He Mixtures near the Superfluid Transition

Guenter Ahlers

*Institut für Festkörperforschung, Kernforschungsanlage, 517 Jülich, Germany, and
Bell Telephone Laboratories, Murray Hill, New Jersey 07974**

and

Frank Pobell

*Institut für Festkörperforschung, Kernforschungsanlage, 517 Jülich, Germany
(Received 10 December 1973)*

We report on measurements of relaxation times for the decay of isothermal concentration gradients in ^3He - ^4He mixtures over the temperature range $10^{-5} \lesssim |\epsilon| \equiv |T/T_\lambda - 1| \lesssim 10^{-2}$. The data yield a mass diffusivity D which diverges when T_λ is approached from higher temperatures. When fitted with $D \propto \epsilon^{-z}$, they give $z = 0.40, 0.36,$ and 0.33 for ^3He concentrations 0.100, 0.208, and 0.399, respectively. The estimated uncertainty for z is ± 0.06 . These results are consistent with theoretical predictions, but differ from experimental results by others.

Recent measurements¹ of mass diffusion in dilute ^3He - ^4He mixtures (^3He concentration $X < 1\%$) seem to imply that the mass diffusivity D remains finite when the superfluid transition temperature T_λ is approached from higher temperatures. This behavior would be in conflict with theoretical predictions.²⁻⁶ We wish to report on measurements of relaxation times for isothermal concentration gradients in ^3He - ^4He mixtures near T_λ . Our results are for molar ^3He concentrations $X = 0.100, 0.208,$ and 0.399 , and for $10^{-5} \lesssim |\epsilon| \equiv |T/T_\lambda - 1| \lesssim 10^{-2}$. Approaching T_λ from higher temperatures, they reveal a divergent D with critical exponents which, within the uncertainties of theory and experiment, agree with the predictions^{3,4} of dynamic scaling^{2,3} and of mode-mode-coupling calculations.⁶

A schematic diagram of our sample cell is shown in the inset of Fig. 1. Most of the mixture is contained in the 0.50-cm-long holes of 0.11 cm diameter in part A . These holes have a center-to-center spacing of 0.14 cm, and yield a 50% transparency. In addition there are two 0.10-cm-high spaces filled with sample, one each above and below the perforated center section of part A . These spaces each contain a capacitor to be used for high-precision measurements of the concentrations of the mixture at the ends of our sample cell. One plate of each capacitor is shown as part B or part B' . The other, shown as a dashed line, was a sheet of 0.012-cm-thick stainless steel, perforated by 0.012-cm-diam holes with a 0.025 cm center-to-center distance (37% transparency).⁷ The spacings between the capacitor

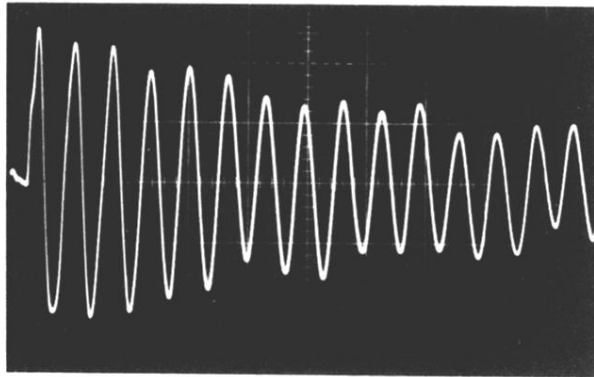


FIG. 1. Response of receiving transducer to a step applied to the transmitting transducer showing the initial transit time and subsequent echoes of fourth sound for a pressure of 25.5 bar and $T/T_c = 0.89$. The receiving bandwidth is $300-10^3$ Hz, the horizontal sweep is 2 msec per main division, and twice the cell length is 5.25 cm.